

Shear mechanism and bearing capacity calculation on steel reinforced concrete special-shaped columns

J.Y. Xue*¹, Z.P. Chen², H.T. Zhao¹, L. Gao¹ and Z.Q. Liu¹

¹College of Civil Engineering, Xi'an University of Architecture and Technology, Xi'an, China

²College of Civil and Architectural Engineering, Guangxi University, Nanning, China

(Received August 18, 2009, Revised August 06, 2012, Accepted September 14, 2012)

Abstract. An experimental study was performed to investigate the seismic performance of steel reinforced concrete (SRC) special-shaped columns. For this purpose, 17 steel reinforced concrete special-shaped column specimens under low-cyclic reversed load were tested, load process and failure patterns of the specimens with different steel reinforcement were observed. The test results showed that the failure patterns of these columns include shear-diagonal compression failure, shear-bond failure, shear-flexure failure and flexural failure. The failure mechanisms and characteristics of SRC special-shaped columns were also analyzed. For different SRC special-shaped columns, based on the failure characteristics and mechanism observed from the test, formulas for calculating ultimate shear capacity in shear-diagonal compression failure and shear-bond failure under horizontal axis and oblique load were derived. The calculated results were compared with the test results. Both the theoretical analysis and the experimental results showed that, the shear capacity of T, L shaped columns under oblique load are larger than that under horizontal axis load, whereas the shear capacity of \perp -shaped columns under oblique load are less than that under horizontal axis load.

Keywords: steel reinforced concrete (SRC); special-shaped columns; shear mechanism; bearing capacity.

1. Introduction

Special-shaped columns, which are shaped as T, L, \perp , are used to supersede rectangular cross sections to avoid convex protruding of frame columns (Yan 2007). By them the building space can be increased, the architecture effects, agility and facility for structure design and utility can also be improved. It is used to set L-shape columns at corner, T-shape at brim, \perp -shape inside the house (Xu 2007, Liu 2009). Columns and infilling wall share unified thickness and hence enlarge the practical area, which make it facilitate for furniture disposing and decoration indoor, and hence be favored by house explorers and owners. More steel area set in steel reinforced concrete (SRC) special-shaped columns and it contributes for the outstanding performance of seismic resistance and bearing capacity of steel reinforced concrete special-shaped columns which are much higher than reinforced concrete special-shaped columns, its outstanding performance also makes them available in wide ranges (Li 2007, Liu 2008). Researchers of Guangxi University studied the mechanism of SRC special-shaped column in advance. Axial and eccentric compression tests on SRC special-shaped columns with T-shape, L-shape and \perp -shape cross sections were initially carried out in 2004 (Chen 2004). Static shear tests on 8 specimens of SRC

* Corresponding author, Ph.D., E-mail: jiayang_xue@163.com

special-shaped columns with T-shape cross section and pseudo-static tests on 4 specimens of SRC special-shaped columns with L-shape cross section were started from 2006 (Liao 2006). It indicates that the bearing capacity and seismic performance of SRC special-shaped column is obviously higher than RC special-shaped column. Researchers of Xi'an University of Technology studied the lattice steel reinforced concrete (LSRC) special-shaped column in 2007. Axial compression tests on 3 specimens of LSRC special-shaped column with L-shape and T-shape cross sections were made, furthermore, static shear tests on 14 specimens of LSRC special-shaped stump column with T-shape cross section were made. The test result also confirms that the bearing capacity of LSRC special-shaped column is much higher. From 2009 to 2010, researchers of Shenyang Jianzhu University had studied the mechanism of axially, one-way eccentrically and two-way eccentrically compressed SRC special-shaped columns which include 18 specimens with T-shape L-shape and + -shape cross sections. The result indicates that all bearing capacity of SRC special-shape column is much higher (Xu 2009). In 2006, researchers of Xi'an University of Architecture and Technology began to study the fundamental theory of SRC special-shaped column, such as thickness of concrete cover and shape steel layout. After that, totally 17 specimens of SRC special-shaped column were tested. Mechanical behavior and seismic performance of the column are analyzed and concluded. Accordingly the flexural and oblique capacity calculation methods are put forward, while the limit value of axial compression ratio and the bond constitutive relationship between shape steel and concrete are suggested. Finally a conclusion that SRC special-shaped column is provided with perfect capability of deformation and energy dissipation is draw. In 2006 researchers of Guangxi University made pseudo-static tests on 6 specimens of SRC special-shaped column-beam side joints which are including 3 plane joint specimens and 3 space joint specimens. Results indicate that the joints exhibit high bearing capacity and ductility. In 2009, based on the study on SRC special-shaped column, researchers of Xi'an University of Architecture and Technology made pseudo-static tests on 17 joint specimens including 4 corner joints, 9 side joints and 4 middle joints. The effects of shape steel layout, axial compression ratio, overhang length of flange and shape steel ratio of joint core on mechanical behavior of the joints are studied. The seismic performance of the joints is analyzed, thus the calculating formulas about joint bearing capacity of crack, shear force and torsion moment are established. Based on the test, the suggestion about construction measures of SRC special-shaped column and the joint is given. The model test of SRC special-shaped column frame can reflect the seismic performance of this new structure system much better. In 2007, pseudo-static test and pseudo-dynamic test on a two story and single span 1/2 scaled plane frame composited by SRC special-shaped column with T-shape cross section and RC beam was accomplished in Guangxi University. The frame model performs a perfect seismic performance, since the shape steel of the column makes a great contribution. The failure mode of the frame presents plastic hinge at beam, which is satisfied with the demand of "strong column-weak beam" (Yang 2009). But the analysis on shear performance of such steel reinforced concrete special-shaped columns is still hanged over (Hidetaka 1984). In this paper, the shear mechanism is revealed and formulas of shear capacity are deduced based on test of steel reinforced concrete special-shaped columns under reversed cyclic loading.

2. Experiment outline

2.1 Specimen design and production

Totally 17 specimens, which included 9 T-shaped, 4 L-shaped and 4 + -shaped columns were designed

(Chen 2007). The parameters in this test were the shape steel, loading direction, axial compression ratio and shear span ratio were used. Shape steel included T-shape steel truss, channel steel truss, and solid shape steel. Loading directions included horizontal axis and oblique axis. Shape steel and cross-sectional geometry of the specimens are shown in Fig. 1. The steel skeletons are shown in Fig. 2. Test parameters are listed in Table 1.

The Q235 steel and HPB235 steel bar were used in producing specimens, of which the mechanical properties are shown in Table 2. Concrete was mixed by forced mixer, and maintained at natural conditions. The mechanical properties of concrete are shown in Table 3. The test setup is shown in Fig. 3. The loading system of force-displacement hybrid control was used in applying the low cyclic reverse load to the SRC special-shaped columns. In the elastic phase, the load was controlled by force, of which the increment was about 20 kN, and one cycle was applied at each level. In the plastic phase, the

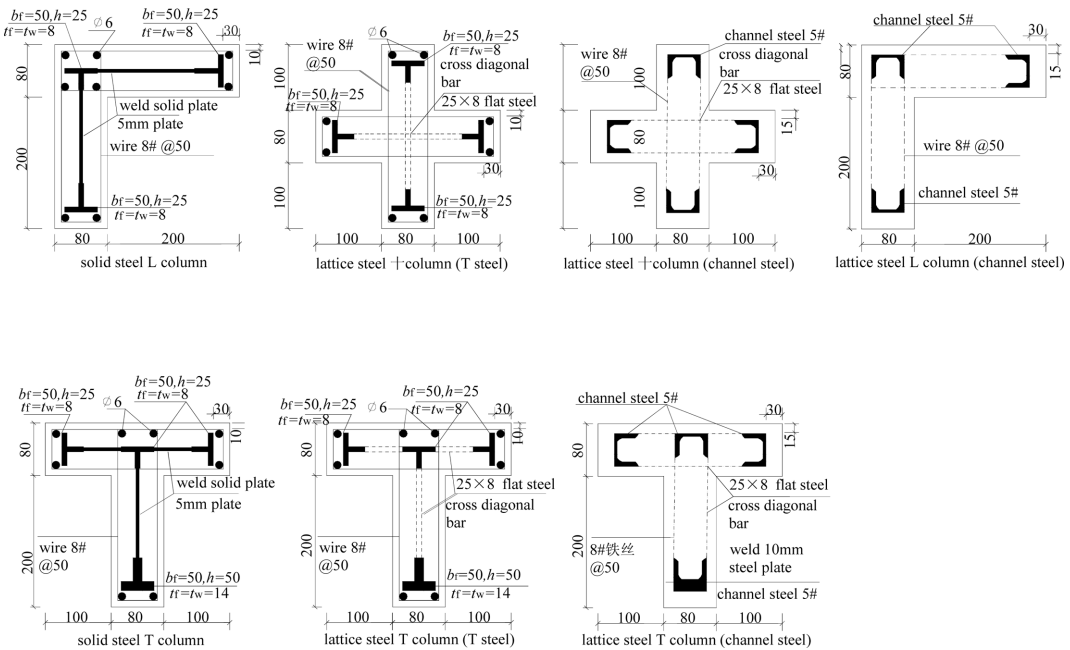


Fig. 1 Geometry and steel details of specimens

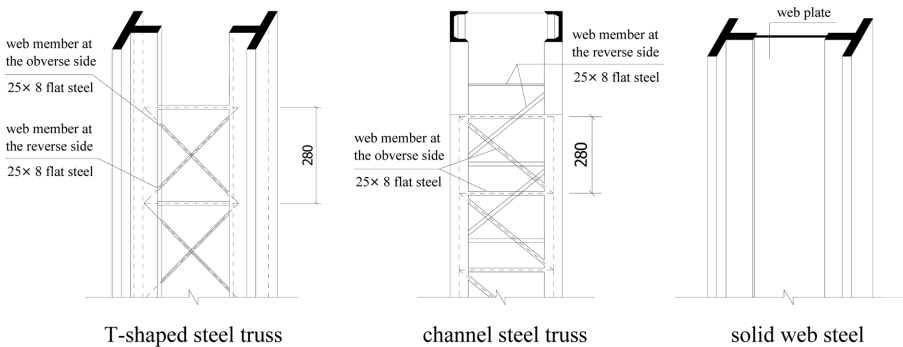


Fig. 2 Steel skeletons

Table 1 Test parameters

Specimen ID	Shape steel	Loading angle	Axial compression ratio n	Shear span ratio λ	Cubic compressive strength $f_{cu}/\text{N}\cdot\text{mm}^{-2}$	$\rho_{ss}/\%$	$\rho_{sw}/\%$
T1	T-shape	along flange	0.3	1	25.48	8.33	3.868
T2	T-shape	along web	0.5	2	27.03	8.33	3.765
T3	T-shape	45°	0.7	2.5	28.09	8.33	3.744
T4	channel	along flange	0.5	2.5	28.09	8.49	3.665
T5	channel	45°	0.7	1	25.48	8.49	3.990
T6	channel	along web	0.3	2	27.03	8.49	3.720
T7	solid	along flange	0.7	2	24.88	11.21	0
T8	solid	45°	0.3	2.5	22.81	11.21	0
T9	solid	along web	0.5	1	27.24	11.21	0
L1	channel	along horizontal axis	0.3	1	27.24	5.39	3.990
L2	channel	45°	0.7	2	27.03	5.39	3.720
L3	solid	along horizontal axis	0.7	2	24.88	7.55	0
L4	solid	45°	0.3	1	25.48	7.55	0
1	T-shape	along horizontal axis	0.5	1	25.48	6.25	1.620
2	T-shape	45°	0.7	2.5	28.09	6.25	3.068
3	channel	along horizontal axis	0.7	2.5	28.09	7.18	3.750
4	channel	45°	0.5	1	27.24	7.18	4.090

Notes: axial compression ratio $n = N/f_c A$, N is axial compressive force, A is area of section, shear span ratio. $\lambda = L/2H$, L is length of specimens, H is height of cross section, ρ_{ss} is ratio of shape steel to concrete area, ρ_{sw} is ratio of diagonal and horizontal steel bar to concrete volume.

loading was controlled by displacement, which progressively increased in accordance with multiple of the yield displacement, and three cycles were applied at each level.

2.2 Failure patterns and mechanisms

Low cyclic reversed load test was carried out on the parallel crosshead equipment. Failure patterns of these specimens can be grouped into four categories: shear-diagonal compression failure, shear-bond failure, shear-flexure failure and flexural failure, which are shown in Fig. 4.

2.2.1 Shear-diagonal compression failure mechanism

Shear-diagonal compression failure occurred mainly on specimens with low shear span ratio ($\lambda = 1$). Its failure procedure could be divided into three stages as elastic, elastic-plastic, and failure. In elastic stage before cracking, deformations of shape steel and concrete were the same. It got into the elastic-plastic stage when cracks appeared. Firstly cross diagonal cracks appeared in the middle segment. The numbers of cracks increased with load increment, and divided surface concrete into small rhombic pieces. With the increment of load, specimens got into the failure stage. Surface concrete was divided into several small short diagonal columns through the formation of several main cross diagonal cracks among the multiple diagonal cracks. Concrete gradually crushed and fell off. The periphery part outside stirrups was crushed firstly and the crushing expanded inside until web or diagonal bars were exposed. In

Table 2 Mechanical properties of steel

Type of steel		Yield stress f_y (MPa)	Tensile stress f_u (MPa)	Elastic modulus E (MPa)	Yield strain μ_s
Shaped steel	Web of 5# channel steel	542.5	667.5	1.952×10^5	2779
	Flange of 5# channel steel	440.0	640.0	2.13×10^5	2065
	25×8 flat steel	385.0	566.7	2.379×10^5	1617
	50×8 flat steel	290.0	435.0	2.162×10^5	1341
	50×10 flat steel	387.5	600.0	1.848×10^5	2096
	50×14 flat steel	277.5	457.5	2.33×10^5	1190
Steel plate	5 mm	352.5	470.0	2.046×10^5	1723
Steel bar	Φ6	360.0	545.0	2.465×10^5	1460
	Φ4	246.7	338.3	1.45×10^5	1701

Table 3 Mechanical properties of concrete

Name of specimen	Cube compressive strength f_{cu} (MPa)	Prism compressive strength f_c (MPa)	Elastic modulus E_c (MPa)	Tensile strength f_t (MPa)
L1, +4, T9	27.240	20.701	2.877×10^4	2.354
T1, +1, L4, T5	25.475	19.361	2.806×10^4	2.251
T3, T4, +2, +3	28.086	21.345	2.909×10^4	2.402
T8	22.813	17.330	2.685×10^4	2.091
L3, T7	24.880	18.908	2.781×10^4	2.216
L2, T2, T6	27.026	20.539	2.869×10^4	2.342

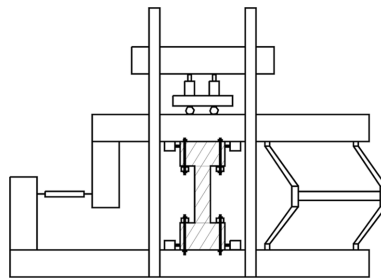


Fig. 3 Test setup



(a) shear-diagonal compression failure



(b) shear-bond failure



(c) flexural failure

Fig. 4 Failure patterns of specimens

the end, web steel yielded, lateral load dropped rapidly and specimens were destroyed. According to the test, strain of shape steel and stirrups were both small in the elastic stage, while shape steel and concrete worked together as a whole element to carry load, and had the same deformation. Concrete quit the work after it cracked. It released elastic energy and transferred it to the web steel it crossed with. Shear stress redistribution occurred, and shear strain of shape steel and stirrups increased obviously and showed nonlinear behavior. When the load reached its peak value, shape steel and stirrups yielded.

2.2.2 Shear-bond failure mechanism

For SRC special-shaped columns with moderate shear span ratio ($\lambda = 2$), shear-bond failure occurred easily. The failure process included the initial appearing of horizontal cracks at both ends of columns, and then cross diagonal cracks appeared in middle segments. The cross diagonal cracks extended with the load increment. They became steep abruptly when extended to the vicinity of steel flanges, and then formed vertical bond cracks. Since then, the bond cracks developed faster than the diagonal cracks, and they interconnect from above to below to form a single vertical bond crack through the height of a column. The crack spited the protective concrete cover, load dropped rapidly and specimens were destroyed. When load reached its peak value, web members of shape steel and stirrup almost approached yield but not yet so.

2.2.3 Shear-flexure failure mechanism

For specimen L4 with low shear span ratio ($\lambda = 2$), which was reinforced with solid web steel and loaded in 45° , shear-flexure failure occurred. Cross diagonal cracks firstly appeared in middle segment. Having the characteristics that large in numbers and small in sizes, these cracks developed and increased in numbers continuously with the increase of loads. In the meantime, horizontal cracks appeared due to moment at both ends. Then with the continuous increase of loads, these horizontal cracks developed faster than the diagonal cracks. At last, vertical cracks appeared at both ends of specimen and concrete was crushed. From failure patterns, it showed that the ultimate load capacity depends on the flexural capacity of normal section. Neither the web steel nor stirrups yielded when failure occurred.

2.2.4 Flexural failure mechanism

Flexural failure occurred in specimens with high shear span ratio ($\lambda = 2.5$). Horizontal flexure cracks or vertical flexure cracks firstly appeared at both ends of specimens. With the increment of load, minor diagonal cracks appeared in some specimens. Failure pattern was shown as the crush of concrete at both ends. Longitudinal steel and bars yielded, but not web steel and stirrups.

3. Failure mechanism of SRC special-shaped columns under oblique loading

Experiments were carried out on T-shape specimens under 0° (along the flange), 45° and 90° (along the web) load, L-shape and $+$ -shape specimens under 0° (along the flange) and 45° load. In polar coordinate system, α denotes the load angle and polar radius denotes characteristic value of shear capacity $V_{u\alpha}/f_t b h_0$. Due to the low-cyclic reversed load, in the directions of 45° (45° and 225°), 0° (0° and 180°) and 90° (90° and 270°), two shear capacities were obtained in each direction. For L-shape and $+$ -shape specimens, the shear capacity at 0° was equal to that at 90° . Based on the test results, all the data points describing shear-diagonal compression failure pattern were depicted in the same polar coordinate system and then the polar coordinate was transferred to rectangular coordinate following the

relations of $x = \rho \sin\alpha$, $y = \rho \cos\alpha$. The results are shown in Fig. 5. The correlation curves of L-shape and T-shape specimens were close to ellipse, and the correlation curves of \perp -shape specimens was close to rhombic (Yin 1990).

Fig. 6 shows shear stress distributions of different SRC special-shaped columns loaded in different directions. It is shown that, for T-shape and L-shape specimens, the maximum shear stress under oblique load was less than that under horizontal axis load. This is mainly due to the enlargement of shear area under oblique load (Hsu 2000). But for \perp -shape specimens, the maximum shear stress under horizontal axis load was less than that under oblique load. This is mainly because that, when specimens were loaded at horizontal axis, the vertical branch locates in the vicinity of centroid of cross section, so the shear stress here decreased. When specimens were under oblique load, the intersection of two vertical branches was in the vicinity of centroid of the cross section, in this place the width of shear-resistance cross section changes abruptly (from double sections to single section to resist shear force), which resulted in the abrupt increase in the maximum shear stress. Although the widths of cross sections with the maximum shear stress in the two load directions were the same, the distance between the critical section and centroid of cross section under horizontal axis load was longer than that under oblique load; therefore its maximum shear stress was less than that under oblique load.

4. Calculation of shear capacity

4.1 Shear capacity of SRC special shaped columns under horizontal axis load

The experiment results show that main failure patterns of SRC special-shaped columns are shear-

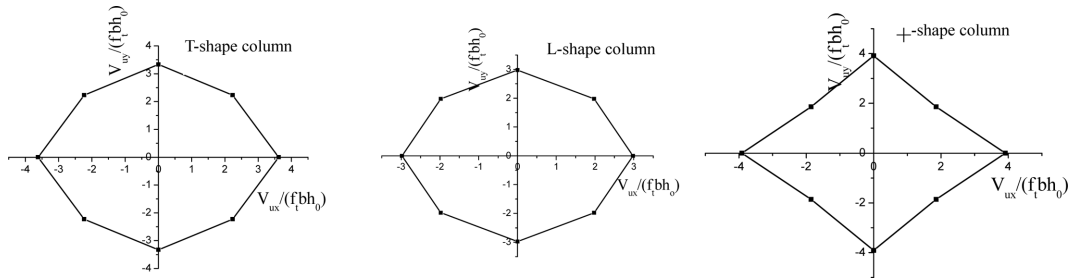


Fig. 5 Relationship between shear-bearing capacity and load direction for SRC special-shaped columns

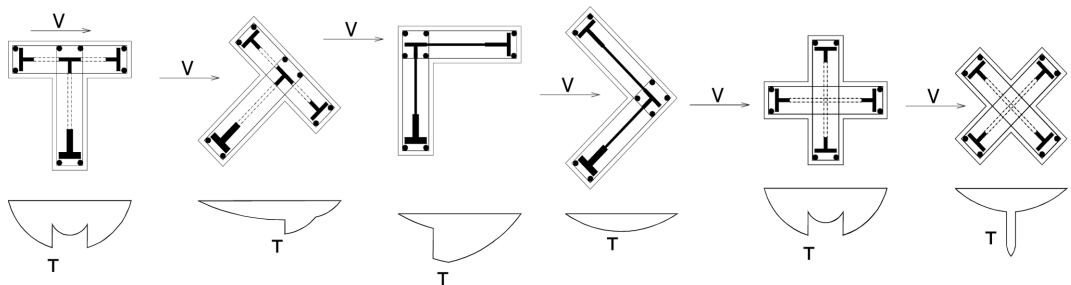


Fig. 6 Shear stress distributions in deferent load direction of SRC special-shaped columns

diagonal compression failure and shear-bond failure. The former one is due to the crush of diagonal concrete short columns divided by diagonal cracks; the latter one is due to the split of concrete outside the steel flanges. According to the aforementioned failure mechanism, web steel yield during the shear-diagonal compression failure, while during the shear-bond failure the bond between shape steel and concrete loses, hence superimposition method can be used to calculate the shear capacity (Zhao 2001, Zhao 2004)

$$V = V_{rc} + V_s \quad (1)$$

Where V_{rc} is the shear force carried by reinforced concrete, V_s is the shear force carried by shape steel.

4.1.1 Calculation of shear capacity in shear-diagonal compression failure

For different shape steel, the shear force taken by shape steel V_s can be calculated using the formula below

4.1.1.1 V_s of solid-web SRC special-shaped columns (Chen 2007)

Before calculation, some assumptions are made as follows: the shear force is born by the web, and the moment is born by the flange and web. The normal stress and shear stress distribute evenly in the web, and obey the yield condition of Mises.

SRC special-shaped column has asymmetric cross section and steel layout, so the simplification as Fig. 7 for the T-shaped column is made, and the L-shaped column and + -shaped column can be made similar simplification.

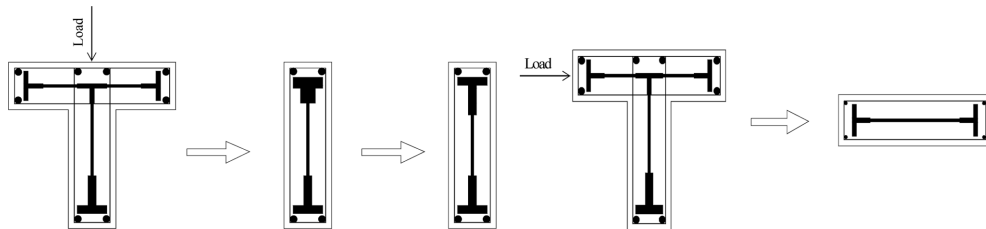
The vertical load of SRC special-shaped column is small usually, so the neutral axis of steel cross section is located at the web, of which the stress distribution is shown as Fig. 8.

From Fig. 6, the equation about axial force (N_s), shear force (V_s) and moment (M_s) can be obtained as Eq. (2).

$$\left(\frac{N_s}{N_{wy}}\right)^2 + \left(\frac{V_s}{V_{sy}}\right)^2 + \left(\frac{M_s}{M_{wy}} - \frac{M_{fy}}{M_{wy}}\right) \sqrt{1 - \left(\frac{V_s}{V_{sy}}\right)^2} = 1 \quad (2)$$

Where $V_{sy} = 1/\sqrt{3} t_w h_w f_s$, $M_{wy} = 1/4 t_w h_w^2 f_s$, $M_{fy} = b_f t_f f_s (h_w + t_f)$, are respectively the ultimate axial force, shear force and moment carried by web and ultimate moment of flanges in the plastic stage of solid shape steel in the column branches paralleling to the load direction.

For the moment (M_s) and shear force (V_s), there is a relationship as Eq. (3).



(a) Load along the web

(b) Load along the flange

Fig. 7 Steel layout simplification for T-shaped column

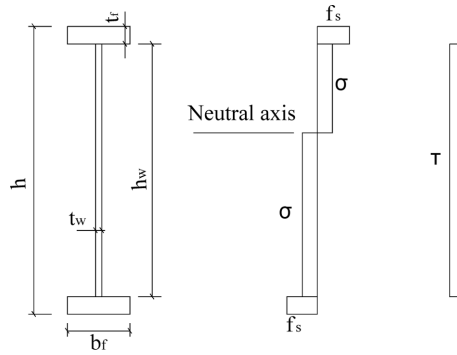


Fig. 8 Stress distribution of steel cross section in plastic state

$$M_s = V_s \cdot \frac{H}{2} \quad (3)$$

Where H is the height of specimens.

Generating Eq. (3) to Eq. (2), Eq. (4) can be obtained.

$$\left(\frac{V_s H}{2M_{wy}} - \frac{M_{fy}}{M_{wy}} \right) \sqrt{1 - \left(\frac{V_s}{V_{sy}} \right)^2} = 1 - \left(\frac{V_s}{V_{sy}} \right)^2 - \left(\frac{N_s}{N_{wy}} \right)^2 \quad (4)$$

Arranging Eq. (4), the Eq. (5) can be obtained.

$$\begin{aligned} & \left(\frac{1}{V_{sy}^4} + \frac{H^2}{4M_{wy}^2 V_{sy}^2} \right) V_s^4 - \frac{HM_{fy}}{M_{wy}^2 V_{sy}^2} V_s^3 - \left(\frac{2}{V_{sy}^2} + \frac{H^2}{4M_{wy}^2} - \frac{M_{fy}^2}{V_{sy}^2 M_{wy}^2} - \frac{2N_s^2}{V_{sy}^2 N_{wy}^2} \right) V_s^2 \\ & + \frac{HM_{fy}}{M_{wy}^2} V_s + \left[1 - \left(\frac{N_s}{N_{wy}} \right)^2 \right]^2 - \frac{M_{fy}^2}{M_{wy}^2} = 0 \end{aligned} \quad (5)$$

For SRC special-shaped column, the compressive stress of steel cross section resulting from the axial force is about $0.05f_y$ to $0.15f_y$, and it is small. In order to simplify the calculation, the influence of axial force on the steel is neglected, that is $N_s = 0$. So the Eq. (6) can be obtained from Eq. (5).

$$V_s = \frac{2HM_{fy}V_{sy}^2 + 2M_{wy}V_{sy}\sqrt{H^2 \cdot V_{sy}^2 - 4(M_{fy}^2 - M_{wy}^2)}}{H^2V_{sy}^2 + 4M_{wy}^2} \quad (6)$$

4.1.1.2 V_s of lattice SRC special-shaped columns

For lattice shape SRC special-shaped columns, treating diagonal members as bent-up steel bars and horizontal members as stirrups, their shear capacity can be calculated using the calculation method for RC members.

$$V_s = f_{sw} A_w \cos \theta + \frac{A_{wh}}{s} f_{sw} h_0 \quad (7)$$

Where f_{sw} is the yield strength of web steel, A_w is the area of diagonal web members in the same cross section, θ is the angle between diagonal web member and horizontal web members which parallel to shear force, A_{wh} is the cross section area of horizontal web members, s is the spacing of horizontal web members along the height of columns, h_0 is the calculated height of the section, let $h_0 = h - a_s$, and a_s is the depth of concrete cover of longitudinal steel.

To define shear capacity V_{rc} of reinforced concrete in SRC special-shaped columns, the current Specification for Design of Concrete Special-Shaped Column Structures (JGJ149-2006) in China can be referred, and the contribution of flanges to the increase of shear capacity should also be considered. Shear capacity of RC segment in SRC special-shaped columns under earthquake action can be defined using the equation below.

$$V_{rc} \leq \frac{1}{\gamma_{RE}} \left(\frac{1.05}{\lambda + 1.0} k \cdot f_t b_c h_0 + f_{yv} \frac{A_{sv}}{s} h_0 + 0.056N \right) \quad (8)$$

Where γ_{RE} is the adjustment coefficient of seismic capacity, λ is the shear span ratio, k is increment factor of shear stress considering the contribution of flanges. Their values are shown in Table 4. According to the distribution of shear stress, shear stress of cross section is calculated with or without the consideration of flanges respectively, and the maximum value is picked, consequently the values of k are defined. f_t is the design axial tensile strength of concrete. b_c and h_0 represent the width and effective height of the calculation section respectively. f_{yv} , A_{sv} and s represent the design yield strength, total section area and spacing of the stirrups respectively. N is the design value of axial compressive force. When $N > 0.3(f_c A_c + f_s A_{ss})$, use $N = 0.3(f_c A_c + f_s A_{ss})$. Here A_c is the net area of concrete cross section.

4.1.2 Calculation of shear capacity in shear-bond failure

The test results show that, for SRC special-shaped columns, when shear-bond failure occurs, web steel and stirrup almost but not yield. Let $\sigma_s = 0.8f_s$ and take it into formulae Eqs. (6) and (7) to calculate V_s . Here the calculation of shear capacity of RC segment V_{rc} is different from that in shear-diagonal compression failure. Although they are all consisted of RC segment and stirrup segment, their expressions are different. V_{rc} here is expressed as

$$V_{rc} = V_c + V_{sv} \quad (9)$$

4.1.2.1 Concrete shear capacity V_c

When the shear-bond failure occurs on SRC special-shaped columns, the force model is shown as

Table 4 k values in different load angle directions

Length to width ratio	T-shape		L -shape	+ -shape
	Loaded along web	Loaded along flange	Loaded along horizontal axis	Loaded along horizontal axis
2.5	1.0007	1.305	1.0007	1.305
3	1.0019	1.208	1.0019	1.208
3.5	1.0073	1.152	1.0073	1.152
4	1.0137	1.117	1.0137	1.117

Fig. 9. The force model of concrete unit body at the split surface is shown as Fig. 10. In Fig. 10, σ_x is the transverse compressive stress of the split surface, and it is provided by the constraint function of stirrup mainly. So σ_x can be expressed as Eq. (10).

$$\sigma_x = \frac{A_{sv}}{bs} \sigma_s \tag{10}$$

Where A_{sv} is the sum of cross section area of stirrup limbs which is parallel to the direction of the shear force. s is the spacing of stirrups along the height of specimen. b is the width of limb of SRC special-shaped column. σ_s is stress of stirrup, and according to the experimental results, it can achieve to f_y .

σ_y is the longitudinal compressive stress of the split surface, which results from the axial force mainly. So σ_y can be expressed as Eq. (11).

$$\sigma_y = \frac{N}{A} \tag{11}$$

Where N is the axial force of specimen. A is the area of cross section of specimen.

τ_{xy} is the longitudinal shear stress of the split surface at both sides of steel flange, and it is τ_1 in Fig. 9. The principal stress of unit body in Fig. 8 can be expressed as Eq. (12).

$$\left. \begin{matrix} \sigma_{max} \\ \sigma_{min} \end{matrix} \right\} = \frac{\sigma_x + \sigma_y}{2} \pm \sqrt{\left(\frac{\sigma_x - \sigma_y}{2}\right)^2 + \tau_{xy}^2} \tag{12}$$

When the maximum principal tensile stress of the split surface achieves to the tensile strength of concrete (f_t), the specimen will be split. So Eq. (12) can be transformed to Eq. (13).

$$\tau_1 = \sqrt{\left(f_t + \frac{\sigma_x + \sigma_y}{2}\right)^2 - \left(\frac{\sigma_x - \sigma_y}{2}\right)^2} \tag{13}$$

Generating Eqs. (10) and (11) to Eq. (13), Eq. (14) can be obtained.

$$\tau_1 = \frac{1}{2} \sqrt{\left(2f_t + \frac{A_{sv}}{bs} f_y + \frac{N}{A}\right)^2 - \left(\frac{A_{sv}}{bs} f_y - \frac{N}{A}\right)^2} \tag{14}$$

In Fig. 9, τ_2 is the bond stress between concrete and steel flange. Based on the previous test results, τ_2 can be expressed as Eq. (15).

$$\bar{\tau}_u = \lambda_{cy} (0.2378 + 0.4480 C_{ss}/d) f_t \tag{15}$$

Where C_s is the thickness of concrete cover for steel flange, d is the height of shape steel section, and λ_{cy} is the degeneration coefficient of the bond stress under reversed load, and according to the test results, $\lambda_{cy} = 0.83$.

From Fig. 9, the follow Equations can be obtained.

$$V_c dx = dM \tag{16}$$

$$dC \cdot j = dM \tag{17}$$

$$dC = (\tau_1(b - b_f) + \tau_2 b_f) dx \tag{18}$$

So

$$V_c = [\tau_1(b - b_f) + \tau_2 b_f] \cdot j \tag{19}$$

Where b_f is the width of shape steel flanges, j is the arm of internal force, which is the distance between midpoint of concrete cover outside the compressive flange and centroid of tensile shape steel in the branch column section paralleling to the direction of shear force.

4.1.2.2 Shear capacity of stirrups V_{sv}

For SRC special-shaped columns, stirrups can not only directly resist shear force but also restrict core concrete to improve bond action between concrete and shape steel. Hence it is necessary to set certain amount of stirrups in such columns. The shear capacity of stirrups is

$$V_{sv} = \sigma_s \frac{A_{sv}}{s} h_0 \tag{20}$$

Where σ_s is the stress of stirrup, from this experimental measurement, $\sigma_s = 0.8f_{yv}$, A_{sv} and s are the total area and the spacing of stirrup at longitudinal direction in branch columns parallel to shear force respectively. h_0 is the calculated height of the section, $h_0 = h - a_s$, a_s is the depth of concrete cover for longitudinal bars.

4.1.3 Comparison between calculated result and test result

From Table 5 we can see that the calculated results agree well with the test results.

4.2 Shear bearing capacity of SRC special shaped columns under oblique load

4.2.1 Shear capacity calculation of the T-shape and L-shape specimens under oblique load

The test results indicate that the correlative curve of the T-shape and L-shape specimens under oblique load is in the shape of ellipse (Maruyama 1984, Wang 2006), so its equation can be written as

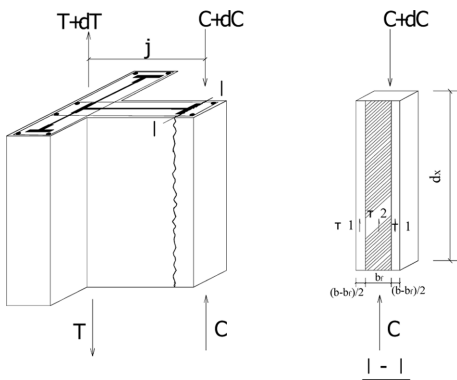


Fig. 9 Force model with shear-bond failure

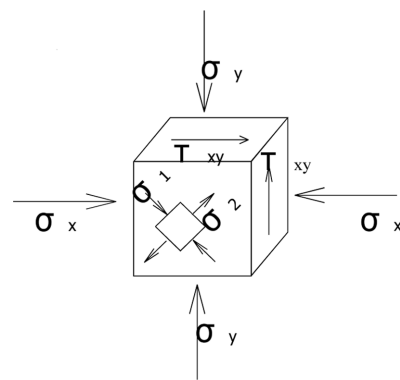


Fig. 10 Force model of concrete unit body

$$\left(\frac{V_x}{V_{ux}}\right)^2 + \left(\frac{V_y}{V_{uy}}\right)^2 = 1 \quad (21)$$

Where V_x is the projection of oblique shear force V on x axis, $V_x = V \cdot \cos\theta$ (θ is the angle between V and x axis), V_y is the projection of oblique shear force V on y axis, $V_y = V \cdot \sin\theta$. V_{ux} and V_{uy} are the shear capacity in x axis and y axis respectively when they are under shear force alone.

In the process of diagonal shear design, assume V is shear design value. If the design is conducted for its projection values V_x and V_y on two main axes and treated like positive direction shear design, the diagonal shear capacity V_u is less than the shear design value V . Therefore shear design under oblique load needs to be conducted excessively in both horizontal axes directions, i.e., increase the design shear resistance values in both horizontal axes directions to $\xi_x V_x$ and $\xi_y V_y$ respectively and treat them as shear design in horizontal axes directions.

Based on the present Code for Design of Concrete Structures (GB50010) in China, shear capacity of SRC special-shaped columns under bi-directional shear load should satisfy the requirements below

$$V_x \leq \frac{V_{ux}}{\xi_x} = \frac{V_{ux}}{\sqrt{1 + \left(\frac{V_{ux}}{V_{uy}} \tan \theta\right)^2}}, \quad V_y \leq \frac{V_{uy}}{\xi_y} = \frac{V_{uy}}{\sqrt{1 + \left(\frac{V_{uy}}{V_{ux}} \cdot \frac{1}{\tan \theta}\right)^2}} \quad (22)$$

V_{ux} , V_{uy} can be calculated using the aforementioned method under single directional shear load.

4.2.2 Shear capacity calculation of the $+$ -shape specimens under oblique load

For $+$ -shape specimens, the test results indicate that shear capacity under load in oblique direction is less than that in horizontal axis direction, and the correlative curve is in the shape of rhombus. Shear stress concentration occurs at the center of the intersection of two column branches, thus it is the weak part of a specimen, as shown in Fig. 5. It is the main part that the cracking from shear-diagonal compression failure and the final failure pattern take place, which has been verified by experimental research. From calculation it is found that the maximum shear stress in the weak part of sections under

Table 5 Comparison of shear capacity between calculated results and test results under horizontal axis load

Specimen ID	Shape steel	Axial compression ratio n	Shear span ratio λ	Concrete tensile strength f_t /MPa	Failure pattern	Measured value V_t /kN	Calculated value V_c /kN	V_t / V_c
T1	T-shape (lattice)	0.3	1	2.25	shear-diagonal compression	175.8	176.5	0.99
T2	T-shape (lattice)	0.5	2	2.34	shear-diagonal compression	168.4	169.8	0.99
T9	solid	0.5	1	2.35	shear-diagonal compression	290.4	239.5	1.21
+1	T-shape (lattice)	0.5	1	2.25	shear-diagonal compression	190.2	182.3	1.04
T6	Channel (lattice)	0.3	2	2.34	shear-bond	151.0	156.4	0.965
L1	Channel (lattice)	0.3	1	2.35	shear-bond	151.5	156.5	0.968

load in oblique direction is identical to that under load in horizontal axis direction without taking the vertical branch column into effect. However, for a + -shape specimen, because its two branches intersect at center, their shear stress distribution in the cross section affects each other. Therefore, taking the increment factor k aforementioned into account, shear capacity under oblique load should be $1/k$ of the shear capacity in any horizontal axis direction, that is:

$$V = V_{ux}/k \quad (23)$$

Where k is the increment factor considering the influence of flange. Values can be found in Table 5. V_{ux} and V_{uy} are shear capacity in the directions of x and y axes respectively when they are under shear load individually. They are equal because of the symmetry of cross sections.

Using the above method, shear capacity of the T-shape, + -shape specimens under oblique load are calculated and compared with actual measured values from experiments (in Table 6). It can be seen that the two results fit very well.

5. Conclusions

(1) Under low-cyclic reversed load, failure patterns of SRC special-shaped columns mainly include shear-diagonal compression failure, shear-bond failure, shear-flexure failure and flexural failure. Shear span ratio is the main influencing factor of failure patterns. The failure pattern which is mainly in the form of shear deformation occurs easily in specimens with low shear span ratio.

(2) Flanges in SRC special-shaped columns can enhance the shear capacity. The degree of enhancement is related with load direction and length to width ratio of column branches, but has nothing to do with the width of branches when the length to width ratio is fixed.

(3) Under oblique load, the shear capacity versus load direction curves are ellipse for T-shape and L-shape columns and rhombic for + -shape columns. For L-shape and T-shape columns, as long as the shear capacities in the two horizontal axes directions are satisfied respectively, the shear capacity in the oblique direction can also be satisfied. But for + -shape columns, because the diagonal shear capacity is slightly less than the shear capacities in two horizontal axes directions, fulfilling the required shear capacities in two horizontal axes directions does not mean the shear capacity in oblique direction is satisfied.

(4) For SRC special shaped columns with different steel reinforcements, based on the shear mechanism in shear-diagonal compression failure and shear-bond failure patterns, formulae for calculating shear capacity under horizontal axis load and oblique load are derived. The calculated results show very good agreement with the test results.

Table 6 Comparison of shear capacity between calculated results and test results under oblique load

Specimen ID	Shape steel	Axial compression ratio n	Shear span ratio λ	Concrete tensile strength f_t /MPa	V_{ux} /kN	V_{uy} /kN	Calculated value V_c /kN	Test value V_t /kN	V_t / V_c
T5	channel truss	0.7	1	2.25	224.4	202.3	237.0	241.6	1.02
4	channel truss	0.5	1	2.35	197.1	197.1	171.1	176.2	1.03

References

- Chen, Z. P. (2007), Study on basic mechanic behavior and seismic performance of steel reinforced concrete special-shaped columns. *Xi'an: Xi'an University of Architecture and Technology*
- Chen, Z. P., Xue, J. Y., and Zhao, H. T. (2007), "Experimental research on seismic behavior of steel reinforced concrete special-shaped columns", *Journal of Building Structures*, **28**(3), 53-61.
- Hidetaka, U. (1984), "Short rectangular RC columns under bilateral loadings", *Journal of Structural Engineering*, **110**(3), 605-618.
- Hsu, H. L. and Wang, C. L. (2000), "Flexural-torsional behavior of steel reinforced concrete members subjected to repeated loading", *J. Earthq. Eng. Struct. Dyn.*, **29**(5), 667-682.
- Li, Z., Zhang, X. F., Guo, Z. Y., and Xu, Kai. (2007), "Experimental study on the mechanical property of steel reinforced concrete short columns of T-shaped cross-section", *Journal of China Civil Engineering*, **40**(1), 1-5.
- Chen, Z. P. (2004), Research on bearing capacity of steel truss SRC asymmetrical T-shaped columns. *Nanning: Guangxi University*.
- Liao, L. P. (2006), Experiment research on seismic behavior of steel reinforced concrete L-shaped section column. *Nan'ning: Guangxi University*.
- Xu, Y. F. (2009), "Experimental study on the biaxial eccentric pressure bearing capacity of Cross-shaped steel reinforced concrete columns", *Journal of Shenyang Architecture University (Natural science edition)*, **25**(1), 100-105.
- Yang, T. (2007), "Research on seismic behavior of frame with T-shaped SRC columns", *Journal of Civil, Architectural & Environmental Engineering*, **31**(2), 33-37.
- Liu, Y., Zhao, H. T., and Xue, J. Y., *et al.* (2008), "Nonlinear analysis of steel reinforced concrete special-shaped column", *Journal of Xi'an University of Architecture and Technology (Natural science edition)*, **40**(3), 312-316, 340.
- Liu, Y., Zhao, H. T., and Xue, J. Y. (2009), "Experimental research on restoring force model of SRC special-shaped columns", *Journal of Earthquake Engineering and Engineering Vibration*, **29**(2), 86-91.
- Maruyama, K., Ramirez, H., and Jirsa, J. O. (1984), "Short RC columns under bilateral load histories", *J. Struct. Eng.*, **110**(2), 120-137.
- Wang, L. J., Wang, T. C., and Wang, S. (2006), "Experimental study on shear behavior of reinforced concrete frame columns under bilateral horizontal loads", *Journal of Building Structures*, **27**(4), 96-102.
- Xu, Y. F., Song, B. F., and Li, G. (2007), "Testing of axial pressure bearing capacity of cross shaped steel reinforced concrete columns", *Journal of Shenyang Jianzhu University (Natural Science)*, **23**(6), 910-913.
- Xue, J. Y. and Zhao, H. T. (2007), "Bond-slip theorem of steel reinforced concrete structures and its applications", *Science Press, Beijing, China*.
- Yan, S. C., Kang, G. Y., and Wang, Y. Q., *et al.* (2007), Comprehension and application of technical specification for concrete structures with special-shaped columns. *Building Industry Press, Beijing, China*.
- Yin, Z. L., Zhang, Y., and Wang, Z. D. (1990), Torsion-resistance. *China Railway Press, Beijing, China*.
- Zhao, H. T. (2001), Steel and concrete composite structures, *Science Press, Beijing, China*.
- Zhao, S. C. (2004), Steel Reinforced concrete composite structure computation theory. *South-West Jiaotong University, Chengdu, China*.